Impacts of coagulation on the appearance time method for sub-3 nm particle growth rate evaluation and their corrections

Runlong Cai[1,2,*], Chenxi Li[3], Xu-Cheng He[2], Chenjuan Deng[4], Yiqun Lu[5], Rujing Yin[4], Chao Yan[1], Lin Wang[5], Jingkun Jiang[4], Markku Kulmala[1,2], Juha Kangasluoma[1,2]

5 [1]Aerosol and Haze Laboratory, Beijing Advanced Innovation Center for Soft Matter Science and Engineering, Beijing University of Chemical Technology, 100029 Beijing, China
[2]Institute for Atmospheric and Earth System Research / Physics, Faculty of Science, University of Helsinki, 00014 Helsinki, Finland
[3]School of Environmental Science and Engineering, Shanghai Jiao Tong University, 200240, China
10 [4]State Key Joint Laboratory of Environment Simulation and Pollution Control, School of Environment, Tsinghua University, 100084 Beijing, China
[5]Shanghai Key Laboratory of Atmospheric Particle Pollution and Prevention (LAP[3]), Department of Environmental Science and Engineering, Fudan University, Shanghai 200433, China

Correspondence to: Runlong Cai (runlong.cai@helsinki.fi)

15 *Keywords*: particle growth rate; coagulation; appearance time; new particle formation; sub-3 nm aerosol, clustering

Abstract. The growth rate of atmospheric new particles is a key parameter that determines their survival probability to become cloud condensation nuclei and hence their impact on the climate. There have been several methods to estimate the new particle growth rate. However, due to the impact of coagulation and measurement uncertainties, it is still challenging to estimate the initial growth rate of sub-3 nm particles, especially in polluted environments with high background aerosol concentrations. In 20 this study, we explore the feasibility of the appearance time method to estimate the growth rate of sub-3 nm particles. The principle of the appearance time method and the impacts of coagulation on the retrieved growth rate are clarified. New formulae in both discrete and continuous spaces are proposed to correct the impacts of coagulation. Aerosol dynamic models are used to test the new formulae. New particle formation in urban Beijing is used to illustrate the importance to consider the impacts of coagulation on sub-3 nm particle growth rate and its calculation. We show that the conventional appearance time method 25 needs to be corrected when the impacts of coagulation sink, coagulation source, and particle coagulation growth are non-negligible compared to the condensation growth. Under the simulation conditions with a constant vapor concentration, the corrected growth rate agrees with the theoretical growth rates. The variation of vapor concentration is found to impact growth rate obtained with the appearance time method. Under the simulation conditions with a varying vapor concentration, the average bias of the corrected 1.5-3 nm particle growth rate range from 6-44%. During the test new particle formation event in 30 urban Beijing, the corrected condensation growth rate of sub-3 nm particles was in accordance with the growth rate contributed by sulfuric acid condensation, whereas the conventional appearance time method overestimated the condensation growth rate of 1.5 nm particles by 80%.

1 Introduction

New particle formation (NPF) is frequently observed in various atmospheric environments (Kulmala et al., 2004;Kerminen et al., 2018;Nieminen et al., 2018;Lee et al., 2019). It contributes significantly to the number concentrations of aerosol and cloud condensation nuclei (CCN) and hence impacts the global climate (Kuang et al., 2009;Kerminen et al., 2012). New particle
5   growth rate is one of the key parameters to characterize NPF events. On the one hand, the newly formed particles (~1 nm) have to survive from coagulation scavenging before they grow to the CCN size (~100 nm). Given the same background aerosol concentration, i.e., the same coagulation loss rate, it is the growth rate that determines the survival probability of new particles (Weber et al., 1997;Lehtinen et al., 2007). Therefore, measuring new particle growth rate accurately contributes to understanding of the impact of NPF on the climate. On the other hand, particle growth rate is a key to investigate the growth
10   mechanisms. Theoretical particle growth rates contributed by condensing vapors are usually compared to measured growth rates to reveal the possible particle growth mechanisms (Ehn et al., 2014;Yao et al., 2018;Mohr et al., 2019). A non-biased and accurate determination of measured growth rates is an important fundament of these comparisons.

Although new particle growth rates are frequently reported in various environments around the world, it remains difficult to retrieve accurate particle growth rates from an ambient dataset. Due to the varying atmospheric conditions, significant
15   Kelvin effect, and size-dependent particle compositions, particle growth rate is a function of both time and particle size. The measured evolution of aerosol size distribution does not directly indicate the size-and-time-resolved growth rate of single particles because one cannot directly track single particles from the size distributions. There are several methods to obtain the size-and-time resolved growth rate by solving aerosol general dynamic equations (GDE, Kuang et al., 2012;Pichelstorfer et al., 2018). However, only few applications of these GDE methods have been reported for particle growth analysis in the real
20   atmosphere (Kuang et al., 2012). The most likely reason is that these GDE methods are sensitive to measurement uncertainties caused by atmospheric instability and instruments, which needs to be solved in future studies.

Apart from solving the GDEs, the widely used methods to estimate particle growth rate are based on finding the representing particle diameter or time. The representing diameter method usually uses the peak diameter of the size distribution of new particles and estimates its increase rate from its temporal evolution. The increase rate of peak diameter is then taken as
25   particle growth rate (Kulmala et al., 2012) after correcting (or sometimes neglecting) the influence of coagulation on the peak shifting (Stolzenburg et al., 2005). During the correction, coagulation is often classified into innermodal coagulation (self-coagulation) and intermodal coagulation (Anttila et al., 2010;Kerminen et al., 2018). The peak diameter is usually obtained by fitting a lognormal function to the measured aerosol size distribution of new particles. With a distinct peak diameter in the growing particle population, this method is theoretically feasible to estimate new particle formation rates. However, the mode
30   fitting is usually tricky, especially when there is no well-defined mode in the growing distribution, either due to the aerosol distribution itself or the measurement uncertainties.

The representing time method estimates the corresponding time for a series of diameters according to a certain criterion and then calculates the growth rate according to the relationship between the diameters and their corresponding time (Dada et

al., 2020). The corresponding time is determined as the time to reach either the maximum concentration (maximum concentration method, Lehtinen and Kulmala, 2003) or a certain proportion of the maximum concentration (appearance time method, Lehtipalo et al., 2014) of a given particle size bin. Previous studies have tested the appearance time under various modeling conditions. Their results indicate that some appearance time methods are able to reproduce the theoretical growth

5   rate within acceptable uncertainties under certain test conditions (Lehtipalo et al., 2014) but not under other test conditions (Olenius et al., 2014;Kontkanen et al., 2016;Li and McMurry, 2018). As shown in the Theory section below, the discrepancy is because that the slope of particle size against their appearance time usually convolves other information (e.g., coagulation) in addition to particle growth.

Determining the growth rate of sub-3 nm particles is more challenging than that of larger particles. Firstly, there are

10   considerable uncertainties in the measured sub-3 nm aerosol size distributions (Kangasluoma et al., 2020) compared to larger-sized particles (e.g., > 10 nm, Wiedensohler et al., 2012). These uncertainties pose a great challenge to the methods based on solving aerosol general dynamic equations. Secondly, during a typical atmospheric NPF event, the sub-3 nm particle size distribution function usually decreases monotonically with the increasing diameter (Jiang et al., 2011b). As a result, the representing diameter method is usually difficult to cover the sub-3 nm size range. In contrast, despite lacking a clear

15   mathematical understanding of the information convolved in the slope of appearance time against particle diameter, the appearance time method is usually favored for sub-3 nm particles and clusters because of the existence of concentration peak of new particles during an atmospheric NPF event. In addition, the appearance time method is not significantly affected by the systematic instrumental uncertainties because the appearance time of each size bin is only determined by the relative signal rather than the absolute particle concentration.

20   Coagulation impacts both particle growth and the grow rate calculation, especially for polluted environments and some chamber studies with high aerosol concentrations. The impact of coagulation on aerosol dynamics has been known since decades ago (e.g., McMurry, 1983). Recent studies discussed the importance of considering coagulation when estimating new particle growth rate (Cai and Jiang, 2017), the influence of transport on measured size distributions (Cai et al., 2018), and primary particle emissions (Kontkanen et al., 2020) under a high aerosol concentration. Similarly, neglecting particle

25   coagulation may cause a bias in the retrieved particle growth rate. Therefore, the coagulation growth has to be considered before investigating the contributions of various condensing vapors to particle growth.

In this study, the feasibility and limitations of the appearance time method are investigated based on theoretical derivations. The impact of coagulation on the retrieved growth rate using the appearance time method is explored and then corrected. Aerosol dynamic models are used to test the conventional and corrected methods. After that, the corrected appearance time

30   method is applied in a typical NPF event in urban Beijing to show the impact of coagulation to growth rate evaluation in the real atmosphere.

2 Theory

2.1 Particle growth rate

Before deriving the formulae for the appearance time method, the definitions of particle growth and coagulation loss have to be clarified to avoid potential misunderstanding. Although widely used in NPF analyses, the exact meanings of these two
5   concepts vary with their applied conditions.

Particle growth rate, by definition, is the rate of increase in particle diameter as a function of time for a given particle. Assuming that there is a sufficient number of particles of the same size and compositions, it is reasonable to neglect the influence of the stochastic effect due to a low particle number and use the expectation of the single-particle growth rate to characterize the growth of the aerosol population with the same size. When there is only one condensing vapor, the formula
10 for the expectation of the single-particle condensation growth rate (referred to as the condensation growth rate below for simplicity) is shown in Eq. 1:

$$\mathrm{GR_{cond}} \ = \ \frac{\Delta d_\mathrm{p}}{\Delta t} \ = \ \beta_{1,\mathrm{p}} N_1 \cdot \left[\sqrt[3]{\left(d_\mathrm{p}^{\ 3} + d_1^{\ 3} \right)} - d_\mathrm{p} \right] \tag{1}$$

where $\mathrm{GR_{cond}}$ is the condensation growth rate (nm s^{-1}) that neglects evaporation, d_p is particle diameter (nm), t is time (s), d_1 is the diameter of the condensing vapor (nm), $\beta_{1,\mathrm{p}}$ is the coagulation coefficient between d_1 and d_p (cm^{-3} s^{-1}), and N_1 is the vapor concentration (cm^{-3}). Particle evaporation is assumed to be negligible and the particle shape is assumed to be spherical
15 both before and after the growth. Note that Eq. 1 is expressed in the discrete form, i.e., it does not assume a continuum particle size ($d_1 \rightarrow 0$). When multiple vapors contribute to particle growth simultaneously, the total condensation growth rate is the sum of the condensation growth rates contributed by every single vapor.

In addition to the condensation of vapors, coagulation also contributes to particle growth. For a given particle with the size of d_p, the coagulation with a particle much smaller than d_p is usually considered as a contribution to its growth. In contrast,
20 the coagulation with a particle much larger than d_p is usually considered as the coagulation loss of particle d_p. We follow this convention to distinguish coagulation growth and loss, i.e., particle coagulation with another particle no larger than itself is taken as coagulation growth and otherwise, it is taken as coagulation loss. Hence, the formula for the expectation of single-particle coagulation growth rate (referred to as the coagulation growth rate for simplicity) in the discrete form is:

$$\mathrm{GR_{coag}} \ = \ \sum_{d_\mathrm{i}=d_\mathrm{min}}^{d_\mathrm{i}=d_\mathrm{p}} \left\{ \beta_{\mathrm{p,i}} N_\mathrm{i} \cdot \left[\sqrt[3]{\left(d_\mathrm{p}^{\ 3} + d_\mathrm{i}^{\ 3} \right)} - d_\mathrm{p} \right] \right\} \tag{2}$$

where $\mathrm{GR_{coag}}$ is the coagulation growth rate (nm s^{-1}), d_min is the minimum particle size (nm), $\beta_{\mathrm{p,i}}$ is the coagulation coefficient
25 (cm^{-3} s^{-1}) between d_p and d_i, and N_i is the concentration (cm^{-3}) of particles with the size d_i. Since both condensation and coagulation contribute to particle growth, the total single-particle growth rate is equal to the sum of $\mathrm{GR_{cond}}$ and $\mathrm{GR_{coag}}$.

When retrieving particle growth rate from the measured aerosol size distributions, the retrieved growth rate is the apparent growth rate. "Apparent" emphasizes that the method does not necessarily guarantee that the retrieved growth rate is equal to the condensation or total growth rate of a single particle or the investigated aerosol population. When using the representing

diameter method, the retrieved apparent growth rate is the increase rate of the peak diameter and it does not directly characterize the growth of any particle(s). For instance, the coagulation loss rate is a function of particle diameter; as a result, the peak diameter shifts towards larger sizes with time because smaller particles are scavenged faster by coagulation than larger particles. Similarly, other size-dependent processes such as condensation and coagulation growth also cause the shift of peak diameter.

5 As a result, the apparent growth rate sometimes needs to be corrected before taken as the total growth rate or the condensation growth rate (Stolzenburg et al., 2005). When using the representing time method, although the retrieved apparent growth rate is close to the condensation growth rate under some modeling conditions (Lehtipalo et al., 2014), their deviation can be significant under other conditions, on which we elaborate in section 4.

2.2 Coagulation sink and source

10 For a given particle, its coagulation with another particle can be classified into coagulation growth and coagulation loss as aforementioned. This classification is based on the Lagrangian specification that tracks the growth of a single particle. In contrast, according to the Eulerian specification that focuses on given particle diameters, each coagulation causes a sink of two particles and a source of one new particle with a larger diameter regardless of the particle sizes. Herein, we define the coagulation sink and source as the loss and production rate for particle size bins in the Eulerian specification. According to

15 these definitions, the coagulation of a particle with another smaller particle is counted as the coagulation sink (in the Eulerian specification) but not as the coagulation loss (in the Lagrangian specification). In accordance with previous studies, we use CoagS (s^{-1}) to represent the sink coefficient (Kulmala et al., 2001) and CoagSrc (cm^{-3} s^{-1}) to represent the production rate due to coagulation (Kuang et al., 2012). Their formulae in the discrete form are given below:

$$\text{CoagS} = \sum_{d_i=d_{min}}^{d_i=d_{max}} \beta_{p,i} N_i \tag{3}$$

$$\text{CoagSrc} = \sum_{d_i=d_{min}}^{d_i^3=d_p^3-d_{min}^3} 0.5\beta_{i,j} N_i N_j \tag{4}$$

where d_{max} is the maximum particle diameter (nm); d_j is defined by $d_j^3 = d_p^3 - d_i^3$; N_i and N_j are the concentrations of d_i and d_j,

20 respectively; and other variables have been introduced above. Note that CoagS and CoagSrc are defined differently and their units are also different. Table 1 summarizes the differences between the definitions in the Lagrangian and Eulerian specifications.

Table 1

2.3 Formulae for the new appearance time method

25 The correction formulae for the appearance time method in the discrete space is:

$$GR_{corr,tot} = GR_{conv} - \left(CoagS + \frac{CoagSrc}{2N_p}\right) \cdot \left[\sqrt[3]{(d_p{}^3 + d_1{}^3)} - d_p\right] \tag{5}$$

$$GR_{conv} = \frac{\Delta d_p}{\Delta t} \tag{6}$$

$$GR_{corr,cond} = GR_{corr,tot} - GR_{coag} \tag{7}$$

where $GR_{corr,tot}$ is the total growth rate (nm s^{-1}) after correcting the impact of both coagulation sink and source; GR_{conv} is the total growth rate (nm s^{-1}) retrieved by the conventional appearance time method; $GR_{corr,cond}$ is the condensation growth rate (nm s^{-1}) after correction; GR_{coag} is the coagulation growth rate (nm s^{-1}); CoagS (s^{-1}) and CoagSrc (cm^{-3} s^{-1}) are the coagulation sink and coagulation source term for d_p, respectively; N_p is the number concentration of particles with the size d_p at its appearance time; Δd_p (nm) is the size difference between two adjacent measured size bins, and Δt (s) is the time difference of the appearance time of these two size bins. Note that coagulation growth is corrected in Eq. 7 but not Eq. 5.

When measuring particle size distribution using size spectrometers, the measured distributions are usually reported in a certain number of sectional bins. Therefore, in addition to the formula in the discrete form (Eq. 5), the correction formula for the appearance time in the sectional form is given below:

$$GR_{corr,tot} = GR_{conv} - \left(CoagS + \frac{CoagSrc}{2N_{[dp,l\ dp,u]}}\right) \cdot \left[\sqrt[3]{(d_p{}^3 + d_1{}^3)} - d_p\right] \tag{8}$$

$$CoagSrc = 0.5 \iint\limits_{d_{p,l}{}^3 \leq d_i{}^3 + d_j{}^3}^{d_i{}^3 + d_j{}^3 < d_{p,u}{}^3} \beta_{i,j} n_i n_j \cdot dlogd_i \cdot dlogd_j \tag{9}$$

where $d_{p,u}$ (nm) and $d_{p,l}$ (nm) are the upper and lower size limits of a given size bin; d_p (nm) is the representative diameter (usually the geometric mean diameter) of this size bin; CoagS is the coagulation sink (s^{-1}) for d_p; CoagSrc is the coagulation source term (cm^{-3} s^{-1}) for the given size bin; $N_{[dp,l\ dp,u]}$ is the measured concentration (cm^{-3}) of the size bin $[d_{p,l}, d_{p,u}]$ at t_p; d_1 is the diameter (nm) of the condensing vapor; and n_i is the aerosol size distribution function (dn_i/dlogd_i, cm^{-3}) for the given size d_i.

The derivation for Eq. 5 is detailed in sections 4.1 and 4.2. The new and conventional appearance time methods are tested using a discrete-sectional model in section 4.3 and a measured atmospheric NPF event in section 4.4.

3 Methods

3.1 Numerical models

A discrete aerosol model and a discrete-sectional aerosol model were used to test the conventional and corrected appearance time methods. The discrete model assumed that new particle formation is driven by the nucleation and condensation of a certain single-component condensing vapor. The vapor concentration was set as a constant. Condensation, coagulation, and external loss were considered in this discrete model. The concentrations of particles up to the size of 100 vapor molecules

(~3.5 nm) were numerically solved using Julia. The theoretical condensation and coagulation growth rates were calculated using Eqs. 1 and 2.

The discrete-sectional model was composed of 30 discrete bins (up to 2.2 nm) and 400 sectional bins (up to 230 nm). The vapor concentration was assumed to follow a normal distribution to simulate its diurnal variation in the real atmosphere. A growth enhancement factor as a function a particle size (Kuang et al., 2010) was used to account for the condensation of multiple vapors. A certain concentration of 100 nm particles was used as background particles and their concentration and size were kept constant during each simulation. The discrete-section model was coded in Matlab and it is detailed in Li and Cai (2020).

The simulation conditions for Figs. 1 and 3-6 are summarized in Table 2. The simulations with varying vapor concentration are summarized in Table A1.

Table 2

3.2 Measurements

The NPF event measured on Feb. 24th, 2018, in urban Beijing was used to test the appearance time method. The measurement site locates on the west campus of the Beijing University of Chemical Technology, which is close to the west 3rd-ring road of Beijing. The aerosol size distributions were measured using a homemade particle size distribution system (PSD, Liu et al., 2016) and a homemade diethylene glycol scanning mobility particle spectrometer (Jiang et al., 2011a;DEG-SMPS, Cai et al., 2017) equipped with a core sampling apparatus (Fu et al., 2019). The sulfuric acid monomer and dimer concentrations were measured using a long chemical ionization time-of-flight mass spectrometers (ToF-CIMS, Aerodyne Research Inc., Jokinen et al., 2012). More details on this measurement site and the instruments have been introduced elsewhere (Cai et al., 2020).

4 Results and discussion

4.1 Appearance time method under ideal conditions

Prior to investigating the impacts of coagulation on the appearance time method, we briefly illustrate the principle of the appearance time method. It can be demonstrated that the appearance time method is able to retrieve the condensation growth rate under ideal conditions. The ideal conditions are:

- The vapor concentration is constant;
- The initial concentrations of new particles are equal to zero;
- Condensation is the only cause of the change in particle concentrations, i.e., there is no coagulation, evaporation, external loss, etc.;
- The condensation rate (i.e., coagulation rate between vapor and particles) is independent of particle diameter.

Under such ideal conditions, the population balance equation for a particle containing i molecules is:

$$\frac{dN_i}{dt} = -\beta N_1 N_i + \beta N_1 N_{i-1} \ (i > 2) \tag{10}$$

where N_1, N_{i-1}, and N_i are the concentrations (cm^{-3}) of the condensing vapor and particles containing i and i-1 monomer molecules, respectively; t is time (s); β is the coagulation coefficient (cm^{-3} s^{-1}) between a vapor molecule and any particle, which is assumed to be independent of the particle size in Eq. 10. For the case i = 2, the last term in Eq. 10 should be modified as $0.5\beta N_1^2$.

5   Solving the differential equations in Eq. 10 yields the analytical solution for N_i:

$$N_i(t) = N_{i,\infty} \times \left[1 - e^{-\beta N_1 t} \sum_{k=0}^{i-2} \frac{(\beta N_1 t)^k}{k!} \right] \tag{11}$$

where $N_{i,\infty}$ is the concentration limit (cm^{-3}) of N_i when t approaches infinite (dN_i/dt = 0) and it is equal to $0.5\beta N_1^2$ (for i > 1) under these ideal conditions.

Figure 1a shows the concentrations of N_i normalized by dividing by their corresponding $N_{i,\infty}$. It can be seen that the distance between two adjacent concentration curves is approximately a constant though these curves are not parallel. Hence,

10   the appearance time method takes the moment that N_i reaches a certain percentage of its maximum value ($N_{i,\infty}$) as its representative time. Previous studies indicate that the 50% size-resolved appearance time method which chooses the certain percent as 50% is more robust against non-ideal conditions compared to using the criterion of other percent values (Lehtipalo et al., 2014). As shown in Fig. 2, an approximate solution of t for $N_i(t) = 0.5N_{i,\infty}$ (referred to as t_i) is:

$$t_i \approx \frac{\ln 2 + i}{\beta N_1} \tag{12}$$

Equation 12 indicates that the slope of particle size in terms of its molecule number versus its appearance time is

15   approximately equal to its condensation growth rate, i.e.,

$$\frac{\Delta i}{\Delta t} = \frac{i - (i-1)}{t_i - t_{i-1}} \approx \beta N_1 = GR_{cond,n} \tag{13}$$

where $GR_{cond,n}$ is the condensation growth rate in terms of the molecule number (s^{-1}). The relationship between $GR_{cond,n}$ herein and GR_{cond} in Eq.1 (which is defined with respect to particle diameter) is $GR_{cond} = GR_{cond,n} \times \Delta d_i$, where Δd_i (nm) is the increase of d_i due to the condensation of one vapor molecule.

Figure 1

20   According to the derivations above, the 50% size-resolved appearance time (referred to as 50% appearance time for short) method is able to retrieve particle growth rate under the given ideal conditions. The slope of particle size versus the appearance time is approximately equal to the condensation growth rate. That is, this slope is mainly determined by condensation growth under these ideal conditions. Note that Eq. 13 is only valid for the 50% appearance time whereas other thresholds to determine the appearance time may cause systematic bias. This bias comes from the non-parallelism of particle concentration curves (see

25   Fig. 1). As shown in Fig. 2, in this test case, the 5% appearance time method overestimates the growth rate by 15% and the 95% appearance time method underestimates the growth rate by 12%. It should be clarified that since these biases are not huge,

it is acceptable to use other thresholds in addition to 50% to reduce the impact of measurement uncertainties in practical applications.

Particle evaporation is assumed to be negligible in the above derivations, yet Fig. 2 indicates that evaporation does not significantly impact the validity of the 50% appearance time method. Assuming a size-independent evaporation rate, E (s^{-1}), t_i

5 is approximately equal to $(\ln 2+i)/(\beta N_1 - E)$, which is bigger than that without evaporation. Meanwhile, considering evaporation, the net condensation growth rate is equal to vapor condensation rate subtracted by particle evaporation rate, i.e., $\beta N_1 - E$. That is, the increase in appearance time agrees with the decrease in the net condensation growth rate. In practice, particle evaporation rate is usually size dependent due to the significant Kelvin effect. The bias caused by this size dependency of evaporation is similar to that of coagulation, which will be shown to have a minor effect below. In addition, the evaporation flux (cm^{-3}s^{-1}) of

10 a given particle containing i molecules is determined by N_{i+1} rather than N_i. As a result, the slope of particle size versus the 50% appearance time may deviate from the net condensation growth rate when i is a small value and there is a non-negligible difference between N_{i+1} and N_i.

Figure 2

Note that the equality between the slope of particle size versus the 50% appearance time and the net condensation growth

15 rate holds only under the above ideal conditions. The following derivations and results will show how the slope is affected by coagulation while maintaining the same condensation growth rate.

4.2 The impacts of coagulation and their corrections

We first show the impact of an external sink to the appearance time method. The external sink is herein referred to as the sink due to coagulation with background particles, wall loss, dilution, transport, etc. For the convenience of comparison with Fig.

20 1a, the external sink is assumed to be temporally independent of particle diameter. The impact of its size dependency will be discussed later. Considering the constant external sink, the population balance equation for N_i is:

$$\frac{dN_i}{dt} = -\beta N_1 N_i - ES N_i + \beta N_1 N_{i-1} \ (i > 2) \tag{14}$$

where ES is the external sink (s^{-1}) and other variables have been introduced in Eq. 10.

Similarly to Eqs. 11 and 12, the approximate solutions for N_i and its corresponding appearance time (t_i) are:

$$N_i(t) = N_{i\infty} \times \left[1 - e^{-(\beta N_1 + ES)t} \sum_{k=0}^{i-2} \frac{[(\beta N_1 + ES)t]^k}{k!} \right] \tag{15}$$

$$t_i \approx \frac{\ln 2 + i}{\beta N_1 + ES} \tag{16}$$

Equations 15 and 16 indicate that the impact of ES to t_i is mathematically equivalent to vapor condensation (βN_1). In the

25 presence of a non-negligible external sink, the particle concentration will approach its limit faster than the scenario without external sink (Fig. 1b). As a result, the slope of particle diameter versus appearance time is affected by both condensation growth and external sink.

Combining Eqs. 1, 13, and 16, the impact of external sink can be readily corrected. The correction formula is:

$$\text{GR}_{\text{EScorr}} = \text{GR}_{\text{conv}} - \text{ES} \cdot \left[\sqrt[3]{(d_p{}^3 + d_1{}^3)} - d_p \right] \qquad (17)$$

where $\text{GR}_{\text{EScorr}}$ is the growth rate (nm s^{-1}) after correcting the external sink, GR_{conv} is the growth rate (nm s^{-1}) retrieved by the conventional appearance time method, and d_1 is the diameter (nm) of the condensing vapor.

As shown in Fig. 3a, with a vapor concentration of 5×10^6 cm^{-3} and an external sink ranging from 1×10^{-3} to 5×10^{-3} s^{-1}, the conventional appearance time method overestimates the condensation growth rate substantially. Such an overestimation caused by mistaking external sink for condensation growth was also reported in previous studies (Olenius et al., 2014;Li and McMurry, 2018). In contrast, the corrected growth rate agrees well with the theoretical condensation growth rate.

Practically, the coagulation coefficient (β) and ES are functions of the particle diameter. For the convenience of illustration, we use the size-dependent coagulation sink, CoagS, as an example to represent the total particle sink due to coagulation, wall loss, dilution, and transport. Similarly to Eq. 15, the approximate analytical solution for N_i with the size-dependent β and CoagS is:

$$N_i(t) \approx N_{i\infty} \times \left\{ 1 - e^{-(\beta_{1,i}N_1 + \text{CoagS}_i)t} \sum_{k=0}^{i-2} \left[\frac{t^k}{k!} \prod_{g=i-k+1}^{i} (\beta_{1,g}N_1 + \text{CoagS}_g) \right] \right\} \qquad (18)$$

where $\beta_{1,i}$ (or $\beta_{1,g}$) is the coagulation coefficient between a vapor molecule and a particle containing i (or g) molecules (cm^{-3} s^{-1}); CoagS_i (or CoagS_g) is the coagulation sink of particles containing i (or g) molecules (s^{-1}); and other variables have been introduced above. Correspondingly, the ES term in Eq. 17 should be replaced with CoagS_i to correct the impact of the size-dependent coagulation sink. When deriving Eq. 18, it is assumed that $\beta_{1,i}N_1 + \text{CoagS}_i$ is close to $\beta_{1,i-1}N_1 + \text{CoagS}_{i-1}$. This approximation is reasonable because both $\beta_{1,i}$ and CoagS_i change gradually with the particle size, yet it introduces minor systematic biases in N_i and its corresponding appearance time.

As shown in Fig. 3b, when $\beta_{1,i}$ and CoagS_i are size dependent, the corrected appearance time method is still able to reproduce the condensation growth rate. It is assumed that the CoagS_i in Fig. 3b is contributed by only the large background particles. Hence, the CoagS_i in Fig. 3b is estimated from the condensation sink (CS) using an empirical formula (Eq. 8 in Lehtinen et al., 2007), where CS indicates the condensation loss rate of the vapor.

Figure 3

In addition to the coagulation with another background particle, the coagulation between two new particles also contributes to the CoagS of both these two particles. As explained in section 2.2, no matter how small the coagulating particle is, the coagulation between a given particle and any other particle should be accounted for in CoagS. This is because the appearance time method is derived in the Eulerian specification and the CoagS is defined with respect to a certain particle diameter rather than with respect to a certain particle. In contrast, when focusing on the survival probability of new particles (Weber et al., 1997;Lehtinen et al., 2007), CoagS should be calculated in the Lagrangian specification, i.e., only the coagulation with a larger particle that causes particle loss should be accounted for. To emphasize the difference between the two definitions

of CoagS, the corrected growth rates using the total (Eulerian) CoagS and the background (Lagrangian) CoagS are compared in Fig. 4. Particle source due to coagulation is not considered in this comparison. A constant concentration of 100 nm particles used as the background particles. The background CoagS refers to the sink due to coagulation with all larger particles, including both the background particles and new particles. The total CoagS is calculated using Eq. 3. Note that due to the contribution

5 of new particles, the total CoagS does not follow a simple decreasing trend with the increasing particle diameter (see Fig. B1 in Cai and Jiang, 2017). Hence, the empirical formula (Lehtinen et al., 2007) to generate a size-dependent CoagS in Fig. 4b should not be used for the total CoagS.

As shown in Fig. 4, the condensation growth rate after correcting the background CoagS is still overestimated. In contrast, the growth rate after correcting the total CoagS agrees with the theoretical growth rate for particles larger than 1.3 nm. For

10 sub-1.3 nm particles, the systematic bias of the growth rate after correcting the total CoagS is mainly caused by the violation of the assumption that $\beta_{1,i}N_1+CoagS_i$ is close to $\beta_{1,i-1}N_1+CoagS_{i-1}$. The size dependence of particle coagulation coefficient under the influence of new particle coagulation increases with decreasing particle size. For instance, under the test conditions, $(\beta_{1,4}N_1+CoagS_4)/(\beta_{1,3}N_1+CoagS_3)$ = 1.12 while $(\beta_{1,50}N_1+CoagS_{50})/(\beta_{1,49}N_1+CoagS_{49})$ = 1.01. As a result, the corrected appearance time method still overestimates the growth rate for sub-1.3 nm particles.

15   **Figure 4**

In addition to CoagS, the impact of coagulation source on the appearance time also needs correction. Adding the coagulation source term to the population balance equation of N_i yields:

$$\frac{dN_i}{dt} = -\beta_{1,i}N_1N_i - CoagS_iN_i + \beta_{1,i-1}N_1N_{i-1} + CoagSrc_i \ (i > 2) \tag{19}$$

$$CoagSrc_i = 0.5\sum_{k=2}^{i-2}\beta_{k,i-k}N_kN_{i-k} \tag{20}$$

where $CoagS_i$ is the coagulation sink (s^{-1}) corresponding to N_i, $CoagSrc_i$ is the coagulation source term (cm^{-3} s^{-1}) corresponding to N_i, and other variables have been introduced above.

20 Since $CoagSrc_i$ is determined by the concentrations of all particles containing 2 to i-2 molecules, it is difficult to obtain an (approximate) analytical solution of Eq. 19. Here we provide an approximation method to correct the impact of coagulation source to the appearance time. Compared to the scenario that coagulation source is neglected, the coagulation source has three impacts on particle growth and its calculation: 1) the coagulation with a smaller particle contributes to particle growth; 2) the coagulation source increases the maximum particle concentrations; 3) the coagulation source shortens the time for particles to

25 reach their maximum concentration.

Impact 1) can be readily corrected using Eq. 7. To correct impacts 2) and 3), we simply assume that $CoagSrc_i$ is a constant during the increasing period of N_i and use the following formulae (see the Appendix for its derivation) to estimate the growth rate. The correction formula has been given in Eq. 5.

The corrected appearance time method (Eqs. 5-7) was tested under various modeling conditions. As the example in Fig.

30 5 indicates, the growth rates estimated using the corrected appearance time method agrees with the theoretical growth rates.

Equation 5 is able to retrieve the growth rate of sub-3 nm particles unless when coagulation source is a governing reason for the change of particle concentration, i.e., $\text{CoagSrc}/2N_p$ is comparable or larger than $\beta_{1,p}N_1$. Under these conditions, CoagSrc may not be a constant and, hence, the approximation of $\text{CoagSrc}/2N_p$ may cause a bias. Fortunately, CoagSrc usually decreases with the increasing particle size due to the decreasing particle concentration. Furthermore, it will be shown in section 4.4 that

5   CoagSrc does not have a major impact on the apparent growth rate even during an intensive atmospheric NPF event. Hence, we consider Eq. 5 as a rough but sufficient formula to correct the impact of coagulation on the appearance time in the real atmosphere.

Figure 5

4.3 The impact of varying vapor concentration

10   In the above analysis, the vapor concentration is assumed to be constant over the whole particle growth period. This assumption may be valid for some chamber experiments; however, the vapor concentration usually follows a diurnal pattern in the real atmosphere. The varying vapor concentration may impact the appearance time and hence the retrieved apparent growth rate. As reported in previous studies (Lehtipalo et al., 2014), the retrieved appearance time is sensitive to the variation of vapor concentration. In the presence of coagulation sink and coagulation growth, it is difficult to correct the impact of the varying

15   vapor concentration. Herein, we use the discrete-sectional model to test the uncertainties of the corrected appearance time method under a varying vapor concentration. The vapor concentration is assumed to follow a normal distribution. The condensation sink is contributed simultaneously by a certain number of 100 nm background particles and the new particles. The growth rate is firstly estimated using the 50% size-resolved appearance time method and then corrected using Eq. 8. Since the vapor concentration varies with time, the retrieved growth rate characterizes particle growth at both different diameters

20   and different time instead of the size-dependent growth at a certain moment. To keep in accordance with the appearance time method, the theoretical condensation and coagulation growth rates of each d_p are calculated at its corresponding t_p.

In general, neglecting the variation of the vapor concentration introduces biases to the appearance time method. As the example shown in Fig. 6 (test No. 8 in Table) indicates, the corrected particle growth rate agrees with the theoretical growth rate better than the conventional growth rate. However, for particles larger than ~5 nm and smaller than ~2 nm, the appearance

25   time method overestimates particle growth rate even after correcting the impact of coagulation in the test case. As summarized in Table A1, the relative discrepancy depends on the exact conditions. The average discrepancy of the corrected appearance time method for 1.5-3 nm particles ranges from 6% to 44% in the test conditions, which is smaller than that of the conventional method.

Although it is difficult to correct the bias due to the varying vapor concentration, one can try to avoid large uncertainties

30   because the bias seems to follow a certain pattern. Compared to the scenario of an increasing vapor concentration, it is found that the discrepancy between the real and retrieved growth rates are usually larger after the peak time of the vapor concentration. As shown in Fig. 6, the appearance time of ~4.9 nm particles is 12 h and a substantial discrepancy between the theoretical and retrieved growth rate is observed for particles larger than 4.9 nm. Fortunately, during a typical atmospheric NPF event, new particles usually grow large before the vapor concentration starts to decrease. To reduce this systematic bias, we suggest using

35   the other methods, e.g., the representing diameter method to estimate particle growth rate when the vapor concentration decreases. For sub-2 nm particles, the appearance time usually convolves other information (e.g., the varying vapor

concentration and the size-dependent coagulation coefficient) in addition to particle growth. Hence, one should be cautious about the sub-2 nm size-resolved growth rate.

Figure 6

4.4 Application in atmospheric measurements

5   A typical intense NPF event measured in urban Beijing is used to test the conventional and corrected appearance time methods. During the event, the peak sulfuric acid concentration was ~6×10^6 cm^{-3} and the average CS for sulfuric acid was 0.024 s^{-1}. The theoretical condensation and coagulation growth rates are calculated using the measured sulfuric acid concentration and aerosol size distribution, respectively. Particle growth due to the uptake of sulfuric acid dimers is herein accounted as the condensation growth. Note that the sum of theoretical condensation and coagulation growth rate is not

10   necessarily equal to the theoretical total growth rate for the measured NPF event. This is because only the condensation of sulfuric acid is considered whereas other vapors may also contribute to new particle growth. The enhancement due to Van der Waals force is considered when calculating the coagulation coefficient (Alam, 1987;Chan and Mozurkewich, 2001;Stolzenburg et al., 2019). The appearance time retrieved from the measured aerosol size distributions was smoothed before estimating the particle growth rate.

15   As shown in Fig. 7, the impacts of particle coagulation are non-negligible compared to particle growth and the grow rate calculation in urban Beijing. On one hand, the conventional appearance time method overestimates particle growth rate for sub-3 nm particles in urban Beijing due to the impact of CoagS. The deviation between the conventional and corrected growth rate decreases with the increasing diameter because CoagS decreases with particle diameter. As illustrated above, the correction for CoagSrc is only an approximation rather than obtained based on solid derivations. However, the negligible impact of

20   CoagSrc on the measured growth rate in urban Beijing indicates that this approximation does not cause a significant bias. Different from coagulation growth which is weighted by particle size, the CoagSrc of d_p is only determined by the number concentrations of particles smaller than d_p (and their coagulation coefficient). Even under such an intense NPF event (with the maximum formation rate exceeding 200 cm^{-3} s^{-1}), the new particle concentration is usually much smaller than the vapor concentration due to the high CoagS and possibly cluster evaporation. Hence, it is sometimes acceptable to neglect the

25   CoagSrc/N_p term in Eqs. 5 and 8 to facilitate calculation. On the other hand, the coagulation with smaller particles enhances particle growth and this enhancement increases with the increasing particle size. This emphasizes that during an intensive NPF event with a high new particle concentration, the condensation growth rate contributed by condensing vapors cannot be taken as the total growth rate that determines the survival probability of new particles.

Figure 7

30   The difference between the measured and theoretical growth rates in Fig. 7 also indicates the growth mechanism of new particles. Considering the uncertainties of the appearance time, the sum of condensation and coagulation flux of sulfuric acid molecules and clusters is approximately equal to the measured particle growth rate for ~3 nm particles, which indicates that sulfuric acid is a governing species that contribute to the initial growth of sub-3 nm particles during the test event. The deviation between the measured growth and theoretical growth for particles larger than ~3 nm indicates that there are other chemical

35   species in addition to sulfuric acid (and the bases to neutralize it) contributing to particle growth. Note that the above discussion is only based on a single case study. Hence, further investigations based on long-term measurements are needed to reveal the growth mechanism in the polluted atmospheric environment.

Summarizing all the analysis above, the growth rate retrieved using the conventional appearance time method may be systematically overestimated due to the impact of coagulation, especially for intensive NPF events in polluted environments. Such an overestimation may be significant for sub-3 nm particles because CoagS increases with the decreasing particle size. In addition, the coagulation growth rate also needs to be corrected before investigating the condensation growth mechanism.

5   For example, in the test case shown in Fig. 7, the retrieved condensation growth rate of 1.5 nm particles using the conventional appearance time method without correcting the impact of CoagS and the coagulation growth rate is overestimated by 80%. Figure 7 also indicates that the impact of CoagS may be negligible for larger particles and clean environments (see also Fig. A1). However, external sinks (e.g., dilution) may also cause an overestimation of the growth rate retrieved using the appearance time method if they are not properly corrected.

10   **5 Conclusions**

The impact of coagulation on the particle growth rate retrieved using the appearance time method was investigated based on theoretical derivations and aerosol dynamics modeling. It was found that the often used 50% size-resolved appearance time method is able to reproduce the condensation growth rate only under the idealized condition without particle coagulation. When using the appearance time method in the real world, coagulation sink, coagulation source, and coagulation growth need

15   to be considered. Equations 5-9 provide a method in both discrete and sectional forms to correct the impacts of coagulation sink and coagulation source to the appearance time method. The feasibility of the corrected method was verified using discrete and discrete-sectional aerosol models. In addition, the variation of vapor concentration was found to impact the appearance time method. The average uncertainties of the corrected 1.5-3 nm particle growth rate for each NPF event were 6-44% in the test cases, respectively. A typical NPF event measured in urban Beijing was used to show the quantitative impacts of

20   coagulation on the retrieved growth rate. The systematic bias of the conventional appearance time method was observed for sub-3 nm particles due to the uncorrected impact of the coagulation sink. In addition, coagulation growth was non-negligible compared to the growth due to sulfuric acid condensation, which emphasizes the importance to distinguish the condensation and total growth rates. During the test event, the apparent growth rate of 1.5 nm particles retrieved using the conventional method was 80% higher than the corrected condensation growth rate, whereas the corrected condensation growth rate was

25   approximately equal to the theoretical growth rate contributed by sulfuric acid condensation.

Appendix

Table A1
Figure A1

30   **Derivation of Eq. 1**

Consider a particle population with a uniform diameter of d_p (nm) and a concentration of N_0. N_0 is assumed to be sufficiently large so that the stochastics in particle growth is negligible. At the initial moment t_0 (s), the mean particle diameter is d_p. During a short time interval dt (s), $\beta_{1,p}N_1N_0dt$ particles collide with the condensing vapor with a diameter of d_1, where $\beta_{1,p}$ is the

coagulation coefficient (cm^3 s^{-1}) and N_1 is the vapor concentration. Hence, the mean diameter ($\overline{d_p}$) weighted by particle number concentration at the moment $t_0 + dt$ is:

$$\overline{d_p}(t_0 + dt) = \beta_{1,p} N_1 dt \sqrt[3]{d_p{}^3 + d_1{}^3} + (1 - \beta_{1,p} N_1 dt) d_p \qquad \text{(Eq. A1)}$$

Comparing $\overline{d_p}(t_0)$ and $\overline{d_p}(t_0 + dt)$ yields the condensation growth rate:

$$GR_{cond} = \frac{\overline{d_p}(t_0 + dt) - \overline{d_p}(t_0)}{dt} = \beta_{1,p} N_1 \cdot \left[\sqrt[3]{(d_p{}^3 + d_1{}^3)} - d_p \right] \qquad \text{(Eq. A2)}$$

The Taylor series of Eq. A2 is:

$$GR_{cond} = \frac{\beta_{1,p} N_1 d_1{}^3}{3 d_p{}^2} + o\left[\beta_{1,p} N_1 d_p \left(\frac{d_1}{d_p}\right)^6 \right] \qquad \text{(Eq. A3)}$$

5   where $o\left[\beta_{1,p} N_1 d_p (d_1/d_p)^6 \right]$ is the Peano form of the remainder. The first term on the right-hand side of Eq. A3 is the formula for particle growth rate in the continuous form and the second term (the remainder) is the difference between the grow rate formula in the continuous and discrete forms (Olenius et al., 2018). When d_p is sufficiently larger than d_1, Eq. A2 is reduced to $\beta_{1,p} N_1 d_1{}^3/(3 d_p{}^2)$.

10   The impacts of coagulation source and their corrections

In this section, we present an approximate derivation for Eq. 5. For the convenience of illustration, particle size and growth rate are characterized using the molecule number rather than particle diameter. Assuming that condensation is the only cause of the change in N_i (Eq. 10), the apparent growth rate is equal to the condensation growth rate, i.e.,

$$GR_{conv} = GR_{app}{}^{(10)} = \beta_{1,i} N_1 \qquad \text{(Eq. A4)}$$

where $GR_{app}{}^{(10)}$ is the apparent growth rate (s^{-1}) of particles containing i molecules and the superscript (10) indicates the
15   population balance assumption in Eq. 10; $\beta_{1,i}$ is the coagulation coefficient (cm^{-3} s^{-1}) between a vapor molecule and particle i; and N_i is the concentration (cm^{-3}) of particle i. N_1 is assumed to be a constant. The conventional appearance time method takes GR_{app} as the growth rate (GR_{conv}) without correction. The source and maximum concentration of N_i are given below:

$$Src^{(10)} = \beta_{1,i-1} N_1 N_{i-1} \qquad \text{(Eq. A5)}$$

$$N_{i,\infty}{}^{(10)} = \frac{\beta_{1,i-1} N_{i-1,\infty}{}^{(10)}}{\beta_{1,i}} = \frac{2\beta_{1,i-1} N_{i-1}}{\beta_{1,i}} \qquad \text{(Eq. A6)}$$

where Src is source for N_i; the $N_{i-1,\infty}$ is the maximum concentration of N_{i-1} (at $t \to +\infty$); N_{i-1} is the concentration of particle i-1 at its appearance time, hence, it is equal to 50% of the maximum concentration of N_{i-1}.

20   Now we consider the scenario with coagulation sink and coagulation source (Eq. 19). The source and maximum concentration of N_i become:

$$Src^{(19)} = \beta_{1,i-1} N_1 N_{i-1} + CoagSrc_i \qquad \text{(Eq. A7)}$$

$$N_{i,\infty}{}^{(19)} = \frac{\beta_{1,i-1}N_1 N_{i-1,\infty}{}^{(19)} + \text{CoagSrc}_i}{\beta_{1,i}N_1 + \text{CoagS}_i} = \frac{2\beta_{1,i-1}N_1 N_{i-1} + \text{CoagSrc}_i}{\beta_{1,i}N_1 + \text{CoagS}_i} \qquad \text{(Eq. A8)}$$

where CoagS_i is the coagulation sink (s^{-1}) corresponding to N_i; and CoagSrc_i is the coagulation source term (cm^{-3} s^{-1}) corresponding to N_i.

As illustrated in the main text, CoagS_i and CoagSrc_i change both Src and $N_{i,\infty}$. The conventional (apparent) growth rate under this scenario can be obtained by accounting for these two aspects, i.e.,

$$
\begin{aligned}
\text{GR}_{\text{conv}} &= \beta_{1,i}N_1 \cdot \frac{N_{i,\infty}{}^{(10)}}{N_{i,\infty}{}^{(19)}} \cdot \frac{\text{Src}^{(19)}}{\text{Src}^{(10)}} \\
&= \beta_{1,i}N_1 \cdot \frac{2\beta_{1,i-1}N_1 N_{i-1,\text{app}}}{\beta_{1,i}N_1} \Big/ \frac{2\beta_{1,i-1}N_1 N_{i-1,\text{app}} + \text{CoagSrc}_i}{\beta_{1,i}N_1 + \text{CoagS}_i} \cdot \frac{\beta_{1,i-1}N_1 N_{i-1,\text{app}} + \text{CoagSrc}_i}{\beta_{1,i-1}N_1 N_{i-1,\text{app}}} \\
&= (\beta_{1,i}N_1 + \text{CoagS}_i) \cdot \left(1 + \frac{\text{CoagSrc}_i}{2\beta_{1,i-1}N_1 N_{i-1,\text{app}} + \text{CoagSrc}_i} \right) \\
&= \beta_{1,i}N_1 + \text{CoagS}_i + \frac{\text{CoagSrc}_i}{N_{i,\infty}} = \beta_{1,i}N_1 + \text{CoagS}_i + \frac{\text{CoagSrc}_i}{2N_{i,\text{app}}}
\end{aligned}
\qquad \text{(Eq. A9)}
$$

According to Eq. A6, the correction formula for the condensation growth rate, GR$_{\text{cond}}$ is:

$$\text{GR}_{\text{cond}} = \text{GR}_{\text{conv}} - \text{CoagS}_i - \frac{\text{CoagSrc}_i}{2N_{i,\text{app}}} \qquad \text{(Eq. A10)}$$

Author contributions. RC, JK, JJ, and MK initialized the study. RC and CL developed the models. RC and X-CH derived the formulae. CD, YL, RY, CY, LW, and JJ performed the measurements and analyzed the data. RC did the simulation and wrote the manuscript with the help of other co-authors.

Code availability. The Julia code for the discrete model is available upon request. The Matlab code for the discrete-sectional model is publicly available in Li and Cai (2020).

Competing interests. The authors declare that they have no conflict of interest.

Acknowledgements. Financial supports from Finnish Academy of Science project (332547, 1325656), UHEL 3-year grant (75284132), National Key R&D Program of China (2017YFC0209503) and Samsung PM$_{2.5}$ SRP are appreciated.

References

Alam, M. K.: The Effect of van der Waals and Viscous Forces on Aerosol Coagulation, Aerosol Science and Technology, 6, 41-52, 10.1080/02786828708959118, 1987.

Anttila, T., Kerminen, V.-M., and Lehtinen, K. E. J.: Parameterizing the formation rate of new particles: The effect of nuclei self-coagulation, Journal of Aerosol Science, 41, 621-636, 10.1016/j.jaerosci.2010.04.008, 2010.

Cai, R., Chen, D.-R., Hao, J., and Jiang, J.: A miniature cylindrical differential mobility analyzer for sub-3 nm particle sizing, Journal of Aerosol Science, 106, 111-119, 10.1016/j.jaerosci.2017.01.004, 2017.

Cai, R., and Jiang, J.: A new balance formula to estimate new particle formation rate: reevaluating the effect of coagulation scavenging, Atmospheric Chemistry and Physics, 17, 12659-12675, 10.5194/acp-17-12659-2017, 2017.

5 Cai, R., Chandra, I., Yang, D., Yao, L., Fu, Y., Li, X., Lu, Y., Luo, L., Hao, J., Ma, Y., Wang, L., Zheng, J., Seto, T., and Jiang, J.: Estimating the influence of transport on aerosol size distributions during new particle formation events, Atmospheric Chemistry and Physics, 18, 16587-16599, 10.5194/acp-18-16587-2018, 2018.

Cai, R., Yan, C., Yang, D., Yin, R., Lu, Y., Deng, C., Fu, Y., Ruan, J., Li, X., Kontkanen, J., Zhang, Q., Kangasluoma, J., Ma, Y., Hao, J., Worsnop, D. R., Bianchi, F., Paasonen, P., Kerminen, V.-M., Liu, Y., Wang, L., Zheng, J., Kulmala, M., and Jiang, J.: Sulfuric acid-

10 amine nucleation under low amine concentrations in the urban atmospheric environment, Nature Communications, under review, 2020.

Chan, T. W., and Mozurkewich, M.: Measurement of the coagulation rate constant for sulfuric acid particles as a function of particle size using tandem di!erential mobility analysis, Journal of Aerosol Science, 32, 321-339, 10.1016/S0021-8502(00)00081-1, 2001.

Dada, L., Lehtipalo, K., Kontkanen, J., Nieminen, T., Baalbaki, R., Ahonen, L., Duplissy, J., Yan, C., Chu, B., Petaja, T., Lehtinen, K., Kerminen, V. M., Kulmala, M., and Kangasluoma, J.: Formation and growth of sub-3-nm aerosol particles in experimental chambers,

15 Nature Protocol, 15, 1013-1040, 10.1038/s41596-019-0274-z, 2020.

Dal Maso, M., Kulmala, M., Lehtinen, K. E., Mäkelä, J. M., Aalto, P., and O'Dowd, C. D.: Condensation and coagulation sinks and formation of nucleation mode particles in coastal and boreal forest boundary layers, Journal of Geophysical Research, 107, D19, 10.1029/2001jd001053, 2002.

Ehn, M., Thornton, J. A., Kleist, E., Sipila, M., Junninen, H., Pullinen, I., Springer, M., Rubach, F., Tillmann, R., Lee, B., Lopez-Hilfiker,

20 F., Andres, S., Acir, I. H., Rissanen, M., Jokinen, T., Schobesberger, S., Kangasluoma, J., Kontkanen, J., Nieminen, T., Kurten, T., Nielsen, L. B., Jorgensen, S., Kjaergaard, H. G., Canagaratna, M., Maso, M. D., Berndt, T., Petaja, T., Wahner, A., Kerminen, V. M., Kulmala, M., Worsnop, D. R., Wildt, J., and Mentel, T. F.: A large source of low-volatility secondary organic aerosol, Nature, 506, 476-479, 10.1038/nature13032, 2014.

Fu, Y., Xue, M., Cai, R., Kangasluoma, J., and Jiang, J.: Theoretical and experimental analysis of the core sampling method: Reducing

25 diffusional losses in aerosol sampling line, Aerosol Science and Technology, 53, 793-801, 10.1080/02786826.2019.1608354, 2019.

Jiang, J., Chen, M., Kuang, C., Attoui, M., and McMurry, P. H.: Electrical Mobility Spectrometer Using a Diethylene Glycol Condensation Particle Counter for Measurement of Aerosol Size Distributions Down to 1 nm, Aerosol Science and Technology, 45, 510-521, 10.1080/02786826.2010.547538, 2011a.

Jiang, J., Zhao, J., Chen, M., Eisele, F. L., Scheckman, J., Williams, B. J., Kuang, C., and McMurry, P. H.: First Measurements of Neutral

30 Atmospheric Cluster and 1–2 nm Particle Number Size Distributions During Nucleation Events, Aerosol Science and Technology, 45, ii-v, 10.1080/02786826.2010.546817, 2011b.

Jokinen, T., Sipilä, M., Junninen, H., Ehn, M., Lönn, G., Hakala, J., Petäjä, T., Mauldin, R. L., Kulmala, M., and Worsnop, D. R.: Atmospheric sulphuric acid and neutral cluster measurements using CI-APi-TOF, Atmospheric Chemistry and Physics, 12, 4117-4125, 10.5194/acp-12-4117-2012, 2012.

35 Kangasluoma, J., Cai, R., Jiang, J., Deng, C., Stolzenburg, D., Ahonen, L. R., Chan, T., Fu, Y., Kim, C., Laurila, T. M., Zhou, Y., Dada, L., Sulo, J., Flagan, R. C., Kulmala, M., Petäjä, T., and Lehtinen, K.: Overview of measurements and current instrumentation for 1-10 nm aerosol particle number size distributions, Journal of Aerosol Science, under review, 2020.

Kerminen, V.-M., Paramonov, M., Anttila, T., Riipinen, I., Fountoukis, C., Korhonen, H., Asmi, E., Laakso, L., Lihavainen, H., Swietlicki, E., Svenningsson, B., Asmi, A., Pandis, S. N., Kulmala, M., and Petäjä, T.: Cloud condensation nuclei production associated with

40 atmospheric nucleation: a synthesis based on existing literature and new results, Atmospheric Chemistry and Physics, 12, 12037-12059, 10.5194/acp-12-12037-2012, 2012.

Kerminen, V.-M., Chen, X., Vakkari, V., Petäjä, T., Kulmala, M., and Bianchi, F.: Atmospheric new particle formation and growth: review of field observations, Environmental Research Letters, 13, 10.1088/1748-9326/aadf3c, 2018.

Kontkanen, J., Olenius, T., Lehtipalo, K., Vehkamäki, H., Kulmala, M., and Lehtinen, K. E. J.: Growth of atmospheric clusters involving

45 cluster–cluster collisions: comparison of different growth rate methods, Atmospheric Chemistry and Physics, 16, 5545-5560, 10.5194/acp-16-5545-2016, 2016.

Kontkanen, J., Deng, C., Fu, Y., Dada, L., Zhou, Y., Cai, J., Dällenbach, K. R., Hakala, S., Kokkonen, T. V., Lin, Z., Liu, Y., Wang, Y., Yan, C., Petäjä, T., Jiang, J., Kulmala, M., and Paasonen, P.: Size-resolved particle number emissions in Beijing determined from measured particle size distributions, Atmospheric Chemistry and Physics Discussions, Submitted, 2020.

50 Kuang, C., McMurry, P. H., and McCormick, A. V.: Determination of cloud condensation nuclei production from measured new particle formation events, Geophysical Research Letters, 36, L09822, 10.1029/2009gl037584, 2009.

Kuang, C., Riipinen, I., Sihto, S. L., Kulmala, M., McCormick, A. V., and McMurry, P. H.: An improved criterion for new particle formation in diverse atmospheric environments, Atmospheric Chemistry and Physics, 10, 8469-8480, 10.5194/acp-10-8469-2010, 2010.

Kuang, C., Chen, M., Zhao, J., Smith, J., McMurry, P. H., and Wang, J.: Size and time-resolved growth rate measurements of 1 to 5 nm

55 freshly formed atmospheric nuclei, Atmospheric Chemistry and Physics, 12, 3573-3589, 10.5194/acp-12-3573-2012, 2012.

Kulmala, M., Dal Maso, M., Mäkelä, J. M., Pirjola, L., Väkevä, M., Aalto, P., Miikkulainen, P., Hämeri, K., and O'dowd, C. D.: On the formation, growth and composition of nucleation mode particles, Tellus, 53, 479-490, 2001.

Kulmala, M., Vehkamäki, H., Petäjä, T., Dal Maso, M., Lauri, A., Kerminen, V.-M., Birmili, W., and McMurry, P. H.: Formation and growth rates of ultrafine atmospheric particles: a review of observations, Journal of Aerosol Science, 35, 143-176, 10.1016/j.jaerosci.2003.10.003, 2004.

Kulmala, M., Petäjä, T., Nieminen, T., Sipilä, M., Manninen, H. E., Lehtipalo, K., Dal Maso, M., Aalto, P. P., Junninen, H., Paasonen, P., Riipinen, I., Lehtinen, K. E., Laaksonen, A., and Kerminen, V.-M.: Measurement of the nucleation of atmospheric aerosol particles, Nature protocols, 7, 1651-1667, 10.1038/nprot.2012.091, 2012.

Lee, S.-H., Gordon, H., Yu, H., Lehtipalo, K., Haley, R., Li, Y., and Zhang, R.: New Particle Formation in the Atmosphere: From Molecular Clusters to Global Climate, Journal of Geophysical Research: Atmospheres, 124, 7098-7146, 10.1029/2018jd029356, 2019.

Lehtinen, K. E. J., and Kulmala, M.: A model for particle formation and growth in the atmosphere with molecular resolution in size, Atmospheric Chemistry and Physics, 3, 251-257, 10.5194/acp-3-251-2003, 2003, 2003.

Lehtinen, K. E. J., Dal Maso, M., Kulmala, M., and Kerminen, V.-M.: Estimating nucleation rates from apparent particle formation rates and vice versa: Revised formulation of the Kerminen–Kulmala equation, Journal of Aerosol Science, 38, 988-994, 10.1016/j.jaerosci.2007.06.009, 2007.

Lehtipalo, K., Leppä, J., Kontkanen, J., Kangasluoma, J., Franchin, A., Wimmer, D., Schobesberger, S., Junninen, H., Petäjä, T., Sipilä, M., Mikkilä, J., Vanhanen, J., Worsnop, D. R., and Kulmala, M.: Methods for determining particle size distribution and growth rates between 1 and 3 nm using the Particle Size Magnifier, Boreal Environment Research, 19, 215-236, 2014.

Li, C., and McMurry, P. H.: Errors in nanoparticle growth rates inferred from measurements in chemically reacting aerosol systems, Atmospheric Chemistry and Physics, 18, 8979-8993, 10.5194/acp-18-8979-2018, 2018.

Li, C., and Cai, R.: Journal of Aerosol Science, in preparation, 2020.

Liu, J., Jiang, J., Zhang, Q., Deng, J., and Hao, J.: A spectrometer for measuring particle size distributions in the range of 3 nm to 10 μm, Frontiers of Environmental Science & Engineering, 10, 63-72, 10.1007/s11783-014-0754-x, 2016.

McMurry, P. H.: New particle formation in the presence of an aerosol: rates, time scales, and sub-0.01 μm size distributions Journal of Colloid and Interface Science, 95, 72-80, 1983.

Mohr, C., Thornton, J. A., Heitto, A., Lopez-Hilfiker, F. D., Lutz, A., Riipinen, I., Hong, J., Donahue, N. M., Hallquist, M., Petaja, T., Kulmala, M., and Yli-Juuti, T.: Molecular identification of organic vapors driving atmospheric nanoparticle growth, Nat Commun, 10, 4442, 10.1038/s41467-019-12473-2, 2019.

Nieminen, T., Kerminen, V.-M., Petäjä, T., Aalto, P. P., Arshinov, M., Asmi, E., Baltensperger, U., Beddows, D. C. S., Beukes, J. P., Collins, D., Ding, A., Harrison, R. M., Henzing, B., Hooda, R., Hu, M., Hõrrak, U., Kivekäs, N., Komsaare, K., Krejci, R., Kristensson, A., Laakso, L., Laaksonen, A., Leaitch, W. R., Lihavainen, H., Mihalopoulos, N., Németh, Z., Nie, W., amp, apos, Dowd, C., Salma, I., Sellegri, K., Svenningsson, B., Swietlicki, E., Tunved, P., Ulevicius, V., Vakkari, V., Vana, M., Wiedensohler, A., Wu, Z., Virtanen, A., and Kulmala, M.: Global analysis of continental boundary layer new particle formation based on long-term measurements, Atmospheric Chemistry and Physics, 18, 14737-14756, 10.5194/acp-18-14737-2018, 2018.

Olenius, T., Riipinen, I., Lehtipalo, K., and Vehkamäki, H.: Growth rates of atmospheric molecular clusters based on appearance times and collision–evaporation fluxes: Growth by monomers, Journal of Aerosol Science, 78, 55-70, 10.1016/j.jaerosci.2014.08.008, 2014.

Olenius, T., Pichelstorfer, L., Stolzenburg, D., Winkler, P. M., Lehtinen, K. E. J., and Riipinen, I.: Robust metric for quantifying the importance of stochastic effects on nanoparticle growth, Sci Rep, 8, 14160, 10.1038/s41598-018-32610-z, 2018.

Pichelstorfer, L., Stolzenburg, D., Ortega, J., Karl, T., Kokkola, H., Laakso, A., Lehtinen, K. E. J., Smith, J. N., McMurry, P. H., and Winkler, P. M.: Resolving nanoparticle growth mechanisms from size- and time-dependent growth rate analysis, Atmospheric Chemistry and Physics, 18, 1307-1323, 10.5194/acp-18-1307-2018, 2018.

Stolzenburg, D., Simon, M., Ranjithkumar, A., Kürten, A., Lehtipalo, K., Gordon, H., Nieminen, T., Pichelstorfer, L., He, X.-C., Brilke, S., Xiao, M., Amorim, A., Baalbaki, R., Baccarini, A., Beck, L., Bräkling, S., Caudillo Murillo, L., Chen, D., Chu, B., Dada, L., Dias, A., Dommen, J., Duplissy, J., El Haddad, I., Finkenzeller, H., Fischer, L., Gonzalez Carracedo, L., Heinritzi, M., Kim, C., Koenig, T. K., Kong, W., Lamkaddam, H., Lee, C. P., Leiminger, M., Li, Z., Makhmutov, V., Manninen, H. E., Marie, G., Marten, R., Müller, T., Nie, W., Partoll, E., Petäjä, T., Pfeifer, J., Philippov, M., Rissanen, M. P., Rörup, B., Schobesberger, S., Schuchmann, S., Shen, J., Sipilä, M., Steiner, G., Stozhkov, Y., Tauber, C., Tham, Y. J., Tomé, A., Vazquez-Pufleau, M., Wagner, A. C., Wang, M., Wang, Y., Weber, S. K., Wimmer, D., Wlasits, P. J., Wu, Y., Ye, Q., Zauner-Wieczorek, M., Baltensperger, U., Carslaw, K. S., Curtius, J., Donahue, N. M., Flagan, R. C., Hansel, A., Kulmala, M., Volkamer, R., Kirkby, J., and Winkler, P. M.: Enhanced growth rate of atmospheric particles from sulfuric acid, Atmospheric Chemistry and Physics Discussions, in review, 10.5194/acp-2019-755, 2019.

Stolzenburg, M. R., McMurry, P. H., Sakurai, H., Smith, J. N., Mauldin, R. L., Eisele, F. L., and Clement, C. F.: Growth rates of freshly nucleated atmospheric particles in Atlanta, Journal of Geophysical Research, 110, D22S05, 10.1029/2005jd005935, 2005.

Wang, Z. B., Hu, M., Sun, J. Y., Wu, Z. J., Yue, D. L., Shen, X. J., Zhang, Y. M., Pei, X. Y., Cheng, Y. F., and Wiedensohler, A.: Characteristics of regional new particle formation in urban and regional background environments in the North China Plain, Atmospheric Chemistry and Physics, 13, 12495-12506, 10.5194/acp-13-12495-2013, 2013.

Weber, R. J., Marti, J. J., McMurry, P. H., Eisele, F. L., Tanner, D. J., and Jefferson, A.: Measurements of new particle formation and ultrafine particle growth rates at a clean continental site, Journal of Geophysical Research: Atmospheres, 102, 4375-4385, 10.1029/96jd03656, 1997.

Wiedensohler, A., Birmili, W., Nowak, A., Sonntag, A., Weinhold, K., Merkel, M., Wehner, B., Tuch, T., Pfeifer, S., Fiebig, M., Fjäraa, A. M., Asmi, E., Sellegri, K., Depuy, R., Venzac, H., Villani, P., Laj, P., Aalto, P., Ogren, J. A., Swietlicki, E., Williams, P., Roldin, P., Quincey, P., Hüglin, C., Fierz-Schmidhauser, R., Gysel, M., Weingartner, E., Riccobono, F., Santos, S., Grüning, C., Faloon, K., Beddows, D., Harrison, R., Monahan, C., Jennings, S. G., O'Dowd, C. D., Marinoni, A., Horn, H. G., Keck, L., Jiang, J., Scheckman, J., McMurry, P. H., Deng, Z., Zhao, C. S., Moerman, M., Henzing, B., de Leeuw, G., Löschau, G., and Bastian, S.: Mobility particle size spectrometers: harmonization of technical standards and data structure to facilitate high quality long-term observations of atmospheric particle number size distributions, Atmospheric Measurement Techniques, 5, 657-685, 10.5194/amt-5-657-2012, 2012.

Yao, L., Garmash, O., Bianchi, F., Zheng, J., Yan, C., Kontkanen, J., Junninen, H., Mazon, S. B., Ehn, M., Paasonen, P., Sipilä, M., Wang, M., Wang, X., Xiao, S., Chen, H., Lu, Y., Zhang, B., Wang, D., Fu, Q., Geng, F., Li, L., Wang, H., Qiao, L., Yang, X., Chen, J., Kerminen, V.-M., Petäjä, T., Worsnop, D. R., Kulmala, M., and Wang, L.: Atmospheric new particle formation from sulfuric acid and amines in a Chinese megacity, Science, 361, 278-281, 10.1126/science.aao4839 2018.

Tables and Figures

Table 1 The impacts of coagulation characterized in the Lagrangian and Eulerian specifications.

	Coagulating with a smaller particle	Coagulating with a larger particle
Lagrangian: tracking individual particles	Coagulation growth (GR_{coag})	Coagulation loss
Eulerian: tracking a given size bin	Coagulation sink (CoagS) for the current bin Coagulation source (CoagSrc) for the next bin	

Table 2 The simulation conditions for Figs. 1 and 3-6. The symbol "√" indicates "yes" and the blank indicates "no".

Figure No.	Constant coagulation coefficient?	External sink?	Coagulation sink?	Coagulation source?	Constant vapor concentration?
1a	√				√
1b & 3a	√	√			√
3b & 4			√		√
5			√	√	√
6			√	√	

Table A1 The mean and maximum relative errors of the conventional and corrected appearance time methods for 1.5-3 nm particles. Conv. and corr. are short for the conventional and corrected methods, respectively. The vapor concentration is assumed to follow a normal distribution with a peak concentration of N_{max} and a standard deviation of σ_t. Background CS characterizes the concentration of 100 nm background particles. The errors are given in relative values. The results of No. 8 test is shown in Fig. 6.

No.	N_{max} (cm^{-3})	σ_t (h)	Background CS (s^{-1})	Mean error conv.	Mean error corr.	Max. error corr.
1	5.0×10^6	2	2×10^{-3}	35%	8%	19%
2	2.0×10^6	2	2×10^{-3}	63%	32%	77%
3	3.5×10^6	2	2×10^{-3}	30%	6%	18%
4	8.0×10^6	2	2×10^{-3}	71%	44%	150%
5	5.0×10^6	1	2×10^{-3}	38%	11%	40%
6	5.0×10^6	3	2×10^{-3}	38%	10%	16%
7	5.0×10^6	4	2×10^{-3}	39%	11%	17%
8	5.0×10^6	2	1×10^{-3}	50%	24%	88%
9	5.0×10^6	2	5×10^{-3}	21%	20%	66%
10	5.0×10^6	2	1×10^{-2}	37%	29%	94%
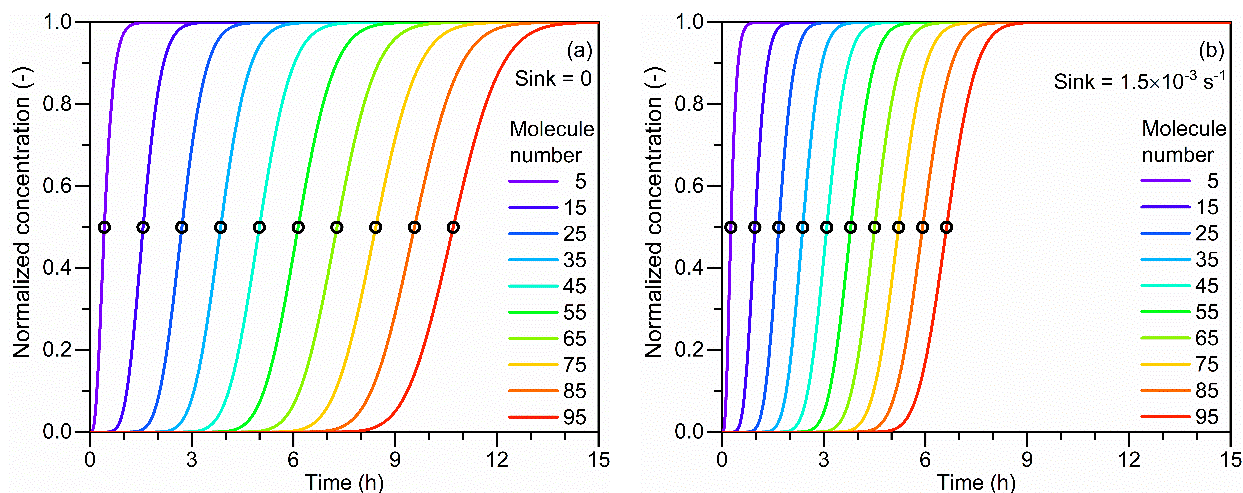
Figure 1 The principle of the appearance time method and the impact of the external sink. (a) Normalized particle concentrations as a function of time. The concentrations are normalized by dividing their corresponding maximum concentrations. The number concentration of the condensation vapor is assumed to be constantly 5×10^6 cm^{-3}. Particle coagulation sink and other sinks are assumed to be negligible. Particle size is indicated by the molecule number contained in every single particle. The open scatters indicate the 50% appearance time corresponding to each particle size. (b) A constant external sink of 1.5×10^{-3} s^{-1} is considered and other simulation conditions are the same as a). Note that due to the assumption of size-independent coagulation coefficient, the appearance time in this figures deviates from that in real new particle formation events.
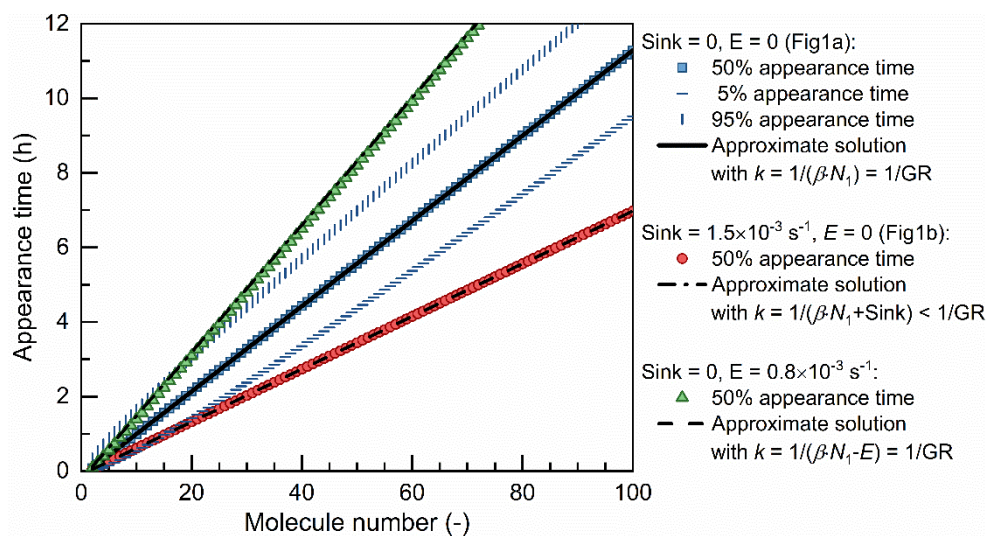
Figure 2 The retrieved appearance time as a function of particle size. The particle size is characterized by the number of molecules contained in each single particle. The scatters are the appearance time retrieved from the simulated concentrations. The curves are the approximate solutions for the 50% appearance time, $t_i = k \times (i + \ln2)$, where k is the slope of the curve (see Eqs. 7 and 11). β is the coagulation coefficient (cm^3 s^{-1}) between vapor and particles, N_1 is the vapor concentration (5×10^6 cm$^-$

[3]), and E is the particle evaporate rate (s^{-1}). When sink = 0, the slope of the approximate solution is equal to the theoretical net condensation growth rate (GR, in terms of the molecule number contained in every single molecule), βN_1-E. However, when sink > 0, the apparent growth rate, βN_1+Sink, is higher than the theoretical condensation growth rate, βN_1.
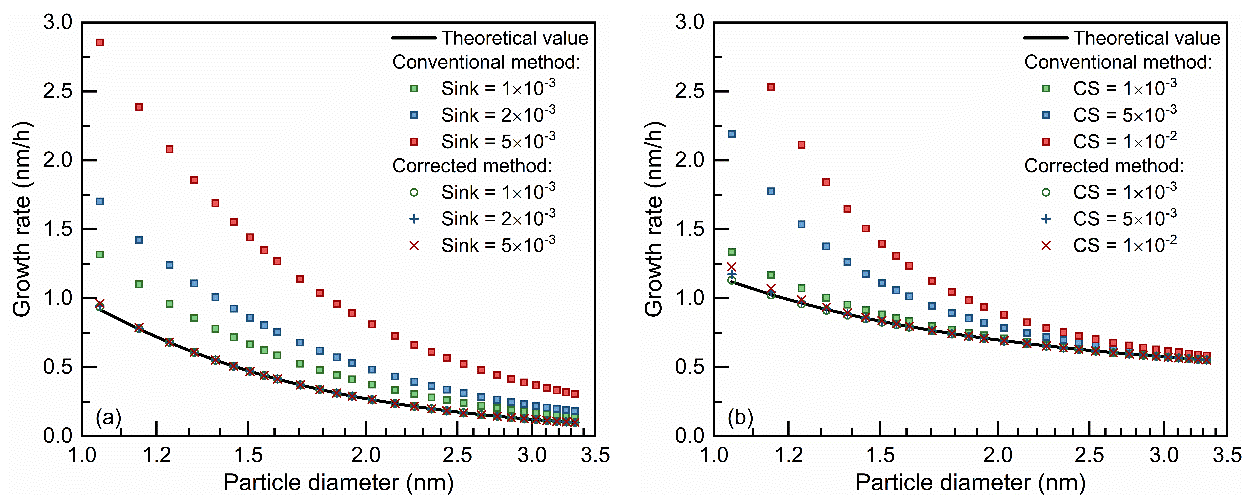
Figure 3 The impact of sinks for the appearance time method and its correction. The theoretical curve is obtained using the condensation rate of the condensing vapor (Eq. 1) and the scatters are obtained using the conventional and corrected appearance time method. The sink is assumed to be independent and dependent of particle diameter in (a) and (b), respectively. The scatters for the corrected method lie on top of each other. The size-dependent coagulation sink in (b) was estimated from the condensation sink (CS) shown in legend using an empirical formula (Lehtinen et al., 2007). The coagulation sink is taken as the input value of the model, hence, the validity of the empirical formula does not affect the accuracy of simulated size distribution or the growth rate. The minor discrepancy among the corrected growth rate comes from the size-dependent particle coagulation coefficient and coagulation sink.
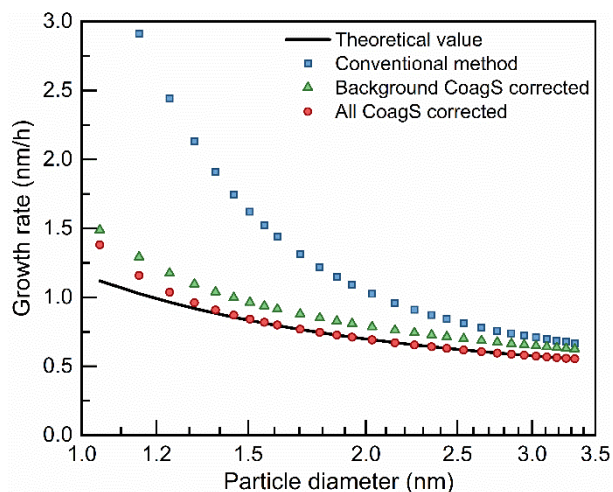
Figure 4 The impact of coagulation sink (CoagS) due to colliding with a smaller particle to the appearance time method. Only the coagulation with a larger particle is accounted for in the correction using the background CoagS.
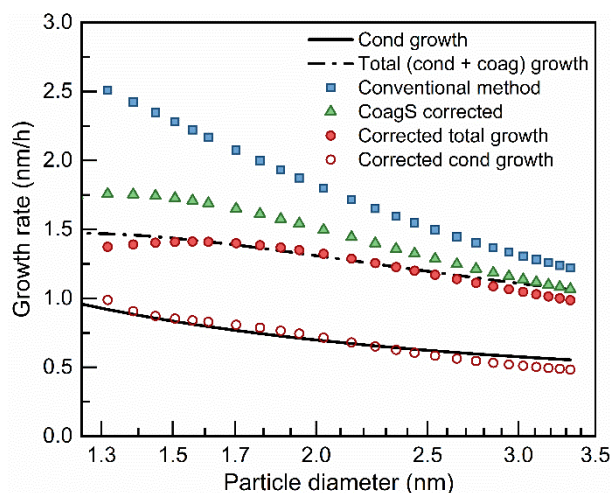
5 **Figure 5** The impact of coagulation sink (CoagS) and coagulation source (CoagSrc) to the appearance time method and the contribution of coagulation growth. Cond and coag are short for condensation and coagulation, respectively. Note that both the solid and dashed lines are theoretical growth rates and their difference is the coagulation growth. Similarly, both the open and filled circles are the measured growth rates after correction and their difference is equal to the coagulation growth rate.
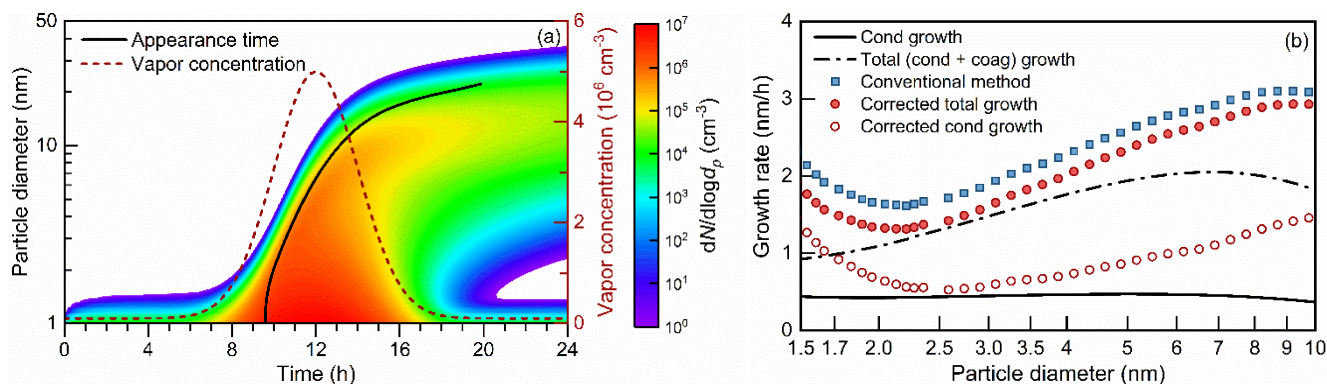
10 **Figure 6** The appearance time method under a varying vapor concentration. The test condition is summarized in Table A1, No. 8. (a) An NPF event simulated using a discrete-sectional aerosol dynamic model. The vapor concentration is assumed to follow a normal distribution (with background value of 10^5 cm^{-3}). The 100-nm background particles are not shown. The particle diameter as a function of the appearance time is shown in the solid line. (b) The theoretical and retrieved particle growth rates.
15 Cond and coag are short for condensation and coagulation, respectively.
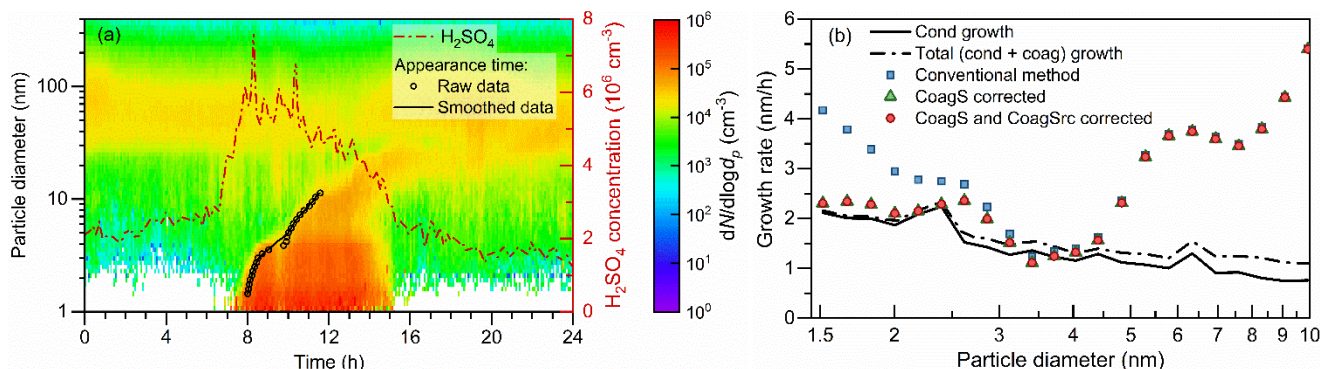
Figure 7 A case study for the appearance time method in the real atmosphere. (a) Aerosol size distribution and H$_2$SO$_4$ concentration during the test NPF day. The event was measured on Feb. 24th, 2018, in urban Beijing. (b) Measured growth rates using the conventional and corrected appearance time methods and the theoretical growth rate contributed by sulfuric acid condensation and particle coagulation. Cond and coag are short for condensation and coagulation, respectively. Note that the theoretical growth rate considers only the sulfuric acid condensation, hence, it may underestimate the overall condensation growth rate contributed by multiple condensing vapors.
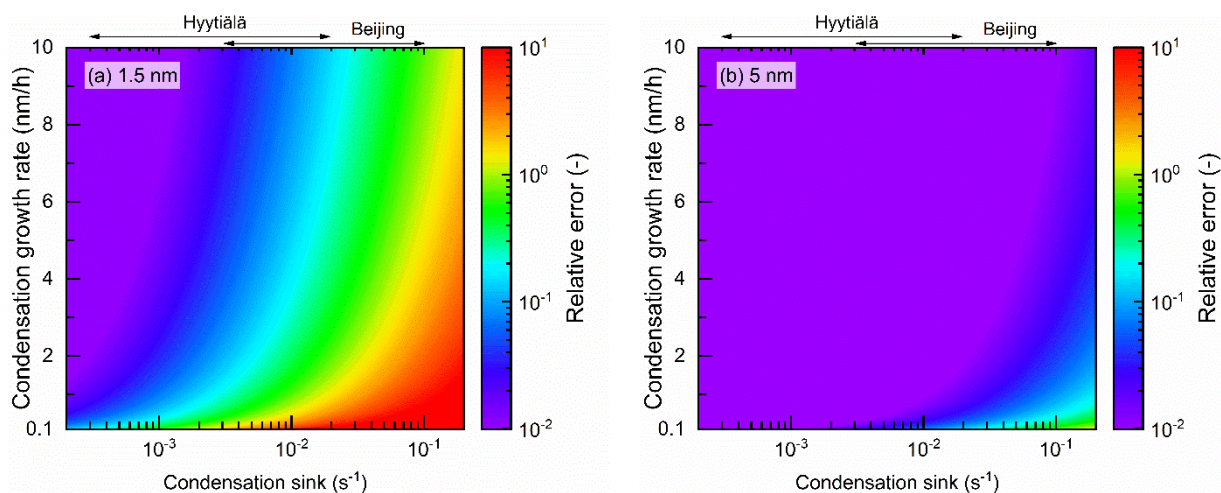
Figure A1 Error of the growth rate retrieved using the conventional appearance time method for (a) 1.5 nm and (b) 5 nm particles. The relative error is defined as (GR$_{conv}$–GR$_{cond}$)/GR$_{cond}$, where GR$_{conv}$ is the growth rate retrieved by the conventional appearance time method and GR$_{cond}$ is the condensation growth rate. Coagulation growth is neglected in this figure. The approximate range of condensation sink in Beijing (Wang et al., 2013) and Hyytiälä (Dal Maso et al., 2002) are marked with arrows, which indicate the typical condensation sink in polluted and clean environments, respectively.